

Measurement of the Branching Fraction for $D(S)^- \rightarrow \phi \pi^-$

CLEO Collaboration

Submitted to Physics Letters B

Stanford Linear Accelerator Center, Stanford University, Stanford, CA 94309

Work supported by Department of Energy contract DE-AC03-76SF00515.

Measurement of the Branching Fraction for $D_s^- \rightarrow \phi\pi^-$

M. Artuso,¹ A. Efimov,¹ M. Gao,¹ M. Goldberg,¹ R. Greene,¹ D. He,¹ N. Horwitz,¹ S. Kopp,¹ G.C. Moneti,¹ R. Mountain,¹ Y. Mukhin,¹ S. Playfer,¹ T. Skwarnicki,¹ S. Stone,¹ X. Xing,¹ J. Bartelt,² S.E. Csorna,² V. Jain,² S. Marka,² A. Freyberger,³ D. Gibaut,³ K. Kinoshita,³ P. Pomianowski,³ S. Schrenk,³ D. Cinabro,⁴ B. Barish,⁵ M. Chadha,⁵ S. Chan,⁵ G. Eigen,⁵ J.S. Miller,⁵ C. O'Grady,⁵ M. Schmidtler,⁵ J. Urheim,⁵ A.J. Weinstein,⁵ F. Würthwein,⁵ D.M. Asner,⁶ M. Athanas,⁶ D.W. Bliss,⁶ W.S. Brower,⁶ G. Masek,⁶ H.P. Paar,⁶ J. Gronberg,⁷ C.M. Korte,⁷ R. Kutschke,⁷ S. Menary,⁷ R.J. Morrison,⁷ S. Nakanishi,⁷ H.N. Nelson,⁷ T.K. Nelson,⁷ C. Qiao,⁷ J.D. Richman,⁷ D. Roberts,⁷ A. Ryd,⁷ H. Tajima,⁷ M.S. Witherell,⁷ R. Balest,⁸ K. Cho,⁸ W.T. Ford,⁸ M. Lohner,⁸ H. Park,⁸ P. Rankin,⁸ J. Roy,⁸ J.G. Smith,⁸ J.P. Alexander,⁹ C. Bebek,⁹ B.E. Berger,⁹ K. Berkelman,⁹ K. Bloom,⁹ D.G. Cassel,⁹ H.A. Cho,⁹ D.M. Coffman,⁹ D.S. Crowcroft,⁹ M. Dickson,⁹ P.S. Drell,⁹ D.J. Dumas,⁹ R. Ehrlich,⁹ R. Elia,⁹ P. Gaidarev,⁹ B. Gittelman,⁹ S.W. Gray,⁹ D.L. Hartill,⁹ B.K. Heltsley,⁹ C.D. Jones,⁹ S.L. Jones,⁹ J. Kandaswamy,⁹ N. Katayama,⁹ P.C. Kim,⁹ D.L. Kreinick,⁹ T. Lee,⁹ Y. Liu,⁹ G.S. Ludwig,⁹ J. Masui,⁹ J. Mevissen,⁹ N.B. Mistry,⁹ C.R. Ng,⁹ E. Nordberg,⁹ J.R. Patterson,⁹ D. Peterson,⁹ D. Riley,⁹ A. Soffer,⁹ C. Ward,⁹ P. Avery,¹⁰ C. Prescott,¹⁰ S. Yang,¹⁰ J. Yelton,¹⁰ G. Brandenburg,¹¹ R.A. Briere,¹¹ T. Liu,¹¹ M. Saulnier,¹¹ R. Wilson,¹¹ H. Yamamoto,¹¹ T. E. Browder,¹² F. Li,¹² J. L. Rodriguez,¹² T. Bergfeld,¹³ B.I. Eisenstein,¹³ J. Ernst,¹³ G.E. Gladding,¹³ G.D. Gollin,¹³ M. Palmer,¹³ M. Selen,¹³ J.J. Thaler,¹³ K.W. Edwards,¹⁴ K.W. McLean,¹⁴ M. Ogg,¹⁴ A. Bellerive,¹⁵ D.I. Britton,¹⁵ R. Janicek,¹⁵ D.B. MacFarlane,¹⁵ P.M. Patel,¹⁵ B. Spaan,¹⁵ A.J. Sadoff,¹⁶ R. Ammar,¹⁷ P. Baringer,¹⁷ A. Bean,¹⁷ D. Besson,¹⁷ D. Coppage,¹⁷ N. Copty,¹⁷ R. Davis,¹⁷ N. Hancock,¹⁷ S. Kotov,¹⁷ I. Kravchenko,¹⁷ N. Kwak,¹⁷ S. Anderson,¹⁸ Y. Kubota,¹⁸ M. Lattery,¹⁸ J.K. Nelson,¹⁸ S. Patton,¹⁸ R. Poling,¹⁸ T. Riehle,¹⁸ V. Savinov,¹⁸ M.S. Alam,¹⁹ I.J. Kim,¹⁹ Z. Ling,¹⁹ A.H. Mahmood,¹⁹ J.J. O'Neill,¹⁹ H. Severini,¹⁹ C.R. Sun,¹⁹ S. Timm,¹⁹ F. Wappler,¹⁹ J.E. Duboscq,²⁰ R. Fulton,²⁰ D. Fujino,²⁰ K.K. Gan,²⁰ K. Honscheid,²⁰ H. Kagan,²⁰ R. Kass,²⁰ J. Lee,²⁰ M. Sung,²⁰ A. Undrus,^{20*} C. White,²⁰ R. Wanke,²⁰ A. Wolf,²⁰ M.M. Zoeller,²⁰ X. Fu,²¹ B. Nemati,²¹ S.J. Richichi,²¹ W.R. Ross,²¹ P. Skubic,²¹ M. Wood,²¹ M. Bishai,²² J. Fast,²² E. Gerndt,²² J.W. Hinson,²² T. Miao,²² D.H. Miller,²² M. Modesitt,²² D. Payne,²² E.I. Shibata,²² I.P.J. Shipsey,²² P.N. Wang,²² M. Yurko,²² L. Gibbons,²³ S.D. Johnson,²³ Y. Kwon,²³ S. Roberts,²³ E.H. Thorndike,²³ C.P. Jessop,²⁴ K. Lingel,²⁴ H. Marsiske,²⁴ M.L. Perl,²⁴ S.F. Schaffner,²⁴ R. Wang,²⁴ T.E. Coan,²⁵ J. Dominick,²⁵ V. Fadeyev,²⁵ I. Korolkov,²⁵ M. Lambrecht,²⁵ S. Sanghera,²⁵ V. Shelkov,²⁵ R. Stroynowski,²⁵ I. Volobouev,²⁵ and G. Wei²⁵

(CLEO Collaboration)

¹*Syracuse University, Syracuse, New York 13244*

²*Vanderbilt University, Nashville, Tennessee 37235*

³*Virginia Polytechnic Institute and State University, Blacksburg, Virginia 24061*

⁴*Wayne State University, Detroit, Michigan 48202*

⁵*California Institute of Technology, Pasadena, California 91125*

⁶*University of California, San Diego, La Jolla, California 92093*

⁷*University of California, Santa Barbara, California 93106*

⁸*University of Colorado, Boulder, Colorado 80309-0390*

⁹*Cornell University, Ithaca, New York 14853*

¹⁰*University of Florida, Gainesville, Florida 32611*

¹¹*Harvard University, Cambridge, Massachusetts 02138*

¹²*University of Hawaii at Manoa, Honolulu, HI 96822*

¹³*University of Illinois, Champaign-Urbana, Illinois, 61801*

¹⁴*Carleton University, Ottawa, Ontario K1S 5B6 and the Institute of Particle Physics, Canada*

¹⁵*McGill University, Montréal, Québec H3A 2T8 and the Institute of Particle Physics, Canada*

¹⁶*Ithaca College, Ithaca, New York 14850*

¹⁷*University of Kansas, Lawrence, Kansas 66045*

¹⁸*University of Minnesota, Minneapolis, Minnesota 55455*

¹⁹*State University of New York at Albany, Albany, New York 12222*

²⁰*Ohio State University, Columbus, Ohio, 43210*

²¹*University of Oklahoma, Norman, Oklahoma 73019*

²²*Purdue University, West Lafayette, Indiana 47907*

²³*University of Rochester, Rochester, New York 14627*

²⁴*Stanford Linear Accelerator Center, Stanford University, Stanford, California, 94309*

²⁵*Southern Methodist University, Dallas, Texas 75275*

Abstract

We present a model-independent measurement of $\mathcal{B}(D_s^- \rightarrow \phi\pi^-)/\mathcal{B}(D^0 \rightarrow K^-\pi^+)$ by partially reconstructing the decay $\overline{B}^0 \rightarrow D^{*+}D_s^{*-}$. Using data collected with the CLEO II detector at CESR, we determine $\mathcal{B}(D_s^- \rightarrow \phi\pi^-)/\mathcal{B}(D^0 \rightarrow K^-\pi^+) = 0.92 \pm 0.20(\text{stat.}) \pm 0.11(\text{syst.})$. Our measurement of $\mathcal{B}(D^0 \rightarrow K^-\pi^+)$ then gives $\mathcal{B}(D_s^- \rightarrow \phi\pi^-) = (3.59 \pm 0.77 \pm 0.48)\%$.

Nearly all the D_s^- branching ratios are measured relative to the $D_s^- \rightarrow \phi\pi^-$ mode. However, this mode is an “uncertain anchor” [1] because its branching fraction has never been reliably measured. The BES experiment has presented $\mathcal{B}(D_s^- \rightarrow \phi\pi^-) = (3.9_{-1.9-1.1}^{+5.1+1.8})\%$ [2], which is based on only two double-tagged D_s events. Estimates for this branching fraction do exist in the references [3,4], but they all make assumptions either about the decay or production of charm mesons, and in some cases, bottom mesons. In this paper, we report the first statistically significant and model independent measurement of this elusive branching fraction. As this result is a direct measurement of the branching fraction it is much more reliable than previous estimates, including those of CLEO [4], which have uncertain model dependent errors.

The data consist of an integrated luminosity of 2.5 fb^{-1} of e^+e^- collisions recorded with the CLEO II detector at the Cornell Electron Storage Ring. The data sample contains about 2.7 million $B\overline{B}$ events taken at center-of-mass energies on the $\Upsilon(4S)$ resonance ($\sqrt{s} \sim 10.58 \text{ GeV}$).

The technique is based on the partial reconstruction of the decay $\overline{B}^0 \rightarrow D^{*+}D_s^{*-}$. This decay is unique because it can be partially reconstructed in two ways. The D_s^{*-} can be fully reconstructed and combined with the soft pion from the decay $D^{*+} \rightarrow D^0\pi^+$ ($N_{D_s^*}$), or the D^{*+} can be fully reconstructed and combined with the soft photon from the decay $D_s^{*-} \rightarrow D_s^-\gamma$ (N_{D^*}). Because the D_s^- is fully reconstructed only in the first instance, $\mathcal{B}(D_s^- \rightarrow \phi\pi^-)$ can be extracted by measuring the efficiency corrected B meson yields using both

*Permanent address: BINP, RU-630090 Novosibirsk, Russia

methods and constraining them to be equal. Although the absolute $D_s^- \rightarrow \phi\pi^-$ branching fraction is not known, the ratios of other D_s^- modes relative to it are, so these can also be used to improve statistics. If the D_s^- and D^0 are reconstructed using $i = 1, \dots, N_{D_s}^{FS}$ and $j = 1, \dots, N_{D^0}^{FS}$ final states,

$$\frac{\mathcal{B}(D_s^- \rightarrow \phi\pi^-)}{\mathcal{B}(D^0 \rightarrow K^-\pi^+)} = \frac{N_{D_s^*}}{\sum_{i=1}^{N_{D_s}^{FS}} R_i(\epsilon \cdot \mathcal{B})_i} \times \frac{\sum_{j=1}^{N_{D^0}^{FS}} R_j(\epsilon \cdot \mathcal{B})_j}{N_{D^*}}, \quad (1)$$

where the quantities R_i and R_j are the D_s^- and D^0 branching ratios relative to $D_s^- \rightarrow \phi\pi^-$ and $D^0 \rightarrow K^-\pi^+$ and where $(\epsilon \cdot \mathcal{B})_i$ and $(\epsilon \cdot \mathcal{B})_j$ are the B meson reconstruction efficiency times sub-mode branching fraction for the D_s^- and D^0 decay modes. A particularly nice feature of this technique is that, since the soft pion and photon are always detected, important systematic errors cancel in the ratio.

When the D_s^{*-} is fully reconstructed (Figure 1a), $\vec{p}_{D_s^{*-}}$ is measured and the constraint $E_B = E_{beam}$ is applied. Although the D^{*+} is not reconstructed here, we can calculate its absolute momentum and one of the angles. If we assume the event is a true $\bar{B}^0 \rightarrow D^{*+}D_s^{*-}$ decay, we can use the constraints $E_B = E_{D^*} + E_{D_s^*}$ and $\vec{p}_B = \vec{p}_{D^*} + \vec{p}_{D_s^*}$, which leads $\cos\theta_{D_s^*D^*} = (p_{D_s^*}^2 + p_{D^*}^2 - p_B^2)/2p_{D_s^*}p_{D^*}$, where $\theta_{D_s^*D^*}$ is the angle between the D_s^{*-} and D^{*+} and where $p_{D^*} = \sqrt{(E_B - E_{D_s^*})^2 - m_{D^*}^2}$. The D^{*+} direction is constrained to lie on a cone of angle $\theta_{D_s^*D^*}$ with respect to the D_s^{*-} direction. The D^{*+} is also constrained to lie on a cone of angle $\theta_{\pi D^*}$ with respect to the soft pion direction where $\cos\theta_{\pi D^*}$ is evaluated in a similar manner. The D^{*+} direction, therefore, corresponds to one of the two intersections of the two cones, which are symmetric with respect to the plane containing the D_s^{*-} and the soft pion. The cosine of the azimuthal angle,

$$\cos\phi_{D^*} = \frac{\cos\theta_{\pi D^*} - \cos\theta_{D_s^*D^*} \cos\theta_{D_s^*\pi}}{\sin\theta_{D_s^*D^*} \sin\theta_{D_s^*\pi}}, \quad (2)$$

measures the location of either solution with respect to this plane and has a very characteristic distribution, satisfying $|\cos\phi_{D^*}| < 1$, for true $\bar{B}^0 \rightarrow D^{*+}D_s^{*-}$ events. When the D^{*+} is fully reconstructed, we calculate $\cos\phi_{D_s^*}$ in a similar manner. Figures 1 (b),(c) show $\cos\phi_{D^*}$ and $\cos\phi_{D_s^*}$ distributions for Monte Carlo signal events. We use these $\cos\phi$ distributions to extract signals.

Three D_s^- decay modes, $D_s^- \rightarrow \phi\pi^-$, K^0K^- and $K^{*0}K^-$, and three D^0 decay modes, $D^0 \rightarrow K^-\pi^+$, $K^-\pi^+\pi^0$ and $\bar{K}^0\pi^+\pi^-$, are used. The D_s^- (D^0) mass is required to lie within 2.5σ of its nominal value. All charged kaon and pion candidates, with the exception of the soft pion, are required to have ionization energy loss and time-of-flight consistent with the expected hypothesis, when this data is available; otherwise no cut is made. We identify ϕ , K^0 , K^{*0} and π^0 candidates using the decay modes $\phi \rightarrow K^+K^-$, $K^0(K_S^0) \rightarrow \pi^+\pi^-$,

$K^{*0} \rightarrow K^-\pi^+$ and $\pi^0 \rightarrow \gamma\gamma$, respectively. We require that the K^+K^- , $\pi^+\pi^-$, $K^-\pi^+$ and $\gamma\gamma$ masses be within $8 \text{ MeV}/c^2$, $10 \text{ MeV}/c^2$, $50 \text{ MeV}/c^2$ and $12 \text{ MeV}/c^2$ of the nominal ϕ , K^0 , K^{*0} and π^0 masses, respectively. For the K_S^0 candidates, the $\pi^+\pi^-$ vertex must be separated from the beam position. For $\gamma\gamma$ combinations which satisfy the π^0 invariant mass cut, a mass-constrained fit is performed to improve the momentum resolution. We require that each photon candidate be found in a single isolated neutral energy cluster with a minimum energy of 30 MeV for $|\cos\theta| < 0.71$ and 50 MeV for $0.71 < |\cos\theta| < 0.95$, where θ is the angle of the shower with respect to the beam-line. At least one photon must lie in the region $|\cos\theta| < 0.71$ and both candidates must have lateral shower shapes consistent with those of photons.

Angular cuts are also used to reduce the combinatoric background. Pseudoscalar to vector-pseudoscalar decays, $D_s^- \rightarrow \phi\pi^-$ and $D_s^- \rightarrow K^{*0}K^-$, follow a $\cos^2\theta_H$ distribution, where θ_H is the angle between either of daughters of the vector particle and the D_s^- direction, both evaluated in the rest-frame of the vector particle. The combinatoric background is flat in $\cos\theta_H$. Therefore, the requirement $|\cos\theta_H| > 0.4$ is imposed on these decays. The decay-angle, θ_D , is the angle between the ϕ evaluated in the D_s^- rest frame and the D_s^- lab direction; for signal events the $\cos\theta_D$ distribution is flat, while the background from random pions is peaked toward $\cos\theta_D=1$. A $\cos\theta_D < 0.9$ cut is imposed for the $D_s^- \rightarrow \phi\pi^-$ decay candidates.

D_s^{*-} and D^{*+} candidates are formed by combining D_s^- and D^0 candidates with soft photons and soft pions. These combinations must satisfy the requirement that the mass-differences, $\Delta M_{D_s^*} = M_{D_s\gamma} - M_{D_s}$ and $\Delta M_{D^*} = M_{D^0\pi^+} - M_{D^0}$, be within 2.5σ of the measured mean values. The typical standard deviations are about $5.3 \text{ MeV}/c^2$ for $\Delta M_{D_s^*}$ and $1.0 \text{ MeV}/c^2$ for ΔM_{D^*} . More stringent requirements are placed on these photons. They are restricted to the barrel region of the detector ($|\cos\theta| < 0.71$), their energies are required to be greater than 110 MeV, and a stricter lateral shape cut is used. In addition, a photon is rejected if it forms a π^0 candidate with any other photon in the event. When the $D^0 \rightarrow K^-\pi^+\pi^0$ mode is used, the D^{*+} signal to background ratio is improved by exploiting the resonant sub-structure of the final state. Candidates are selected from high probability regions of the Dalitz plot. D^{*+} candidates are rejected if they are consistent with coming from $B \rightarrow D^{*+}\ell\nu$ decay.

When the D_s^{*-} is fully reconstructed, we consider two kinds of backgrounds, fake D_s^{*-} 's combined with either true or random pions, and random pions combined with the true D_s^{*-} 's. We use a Monte Carlo simulation, which includes both $B\overline{B}$ and continuum events, to obtain the $\cos\phi_{D^*}$ distribution for both backgrounds. We use data to obtain the normalization for the fake D_s^{*-} contribution.

To obtain the normalization for the fake D_s^{*-} background in the D_s^{*-} signal region, we use $\Delta M_{D_s^*}$ sidebands ($60 < \Delta M_{D_s^*} < 90$, $170 < \Delta M_{D_s^*} < 220$ MeV/ c^2) from the Monte Carlo and the data as control samples. First, we divide the Monte Carlo sideband into two samples, one with true pions from D^{*+} decay and the one with random pions. The first sample tends to peak in the signal region of the $\cos \phi_{D^*}$ distribution, when the soft photon is fake and the D_s^- is true. Since the Monte Carlo does not necessarily produce the two contributions with the correct ratio, the ratio of these two is obtained from data. We fit the data sideband distribution using these two Monte Carlo sideband distributions with both normalizations floated as shown in figure 2. This procedure gives the absolute normalization as well as the ratio of the normalizations for the two fake D_s^{*-} backgrounds.

When the D^{*+} is fully reconstructed, we also consider two kinds of backgrounds, fake D^{*+} 's and random photons with the true D^{*+} 's. We use the Monte Carlo simulation to obtain $\cos \phi_{D_s^*}$ distribution for the backgrounds. For the fake D^{*+} background, we use the same procedure to obtain the normalization as was used for the fake D_s^{*-} background. Since the random photon background is a dominant background source and is rising in the signal region, we pay particular attention to its shape. Since the background shape depends on the photon energy spectrum and on the D^{*+} momentum spectrum, we compare these distributions between the data and Monte Carlo. In particular, we study the E_γ and $P_{D^{*+}}$ distributions, for photons and D^{*+} 's used in a candidate combination, but after reversing the direction of all soft photon candidates. The reversed photon distribution provides a good approximation for the isotropically distributed random photon background; the majority (75%) of the random photon background is due to photons from the decay of the other B meson in the event, and is therefore isotropic. We compare the data and Monte Carlo distributions by calculating their ratio in each bin. The points in figure 3 show this ratio as a function of E_γ ; we observe a systematic trend. We fit the shape to a second order polynomial function to obtain a correction function. The solid line in figure 3 shows the fit. When filling the $\cos \phi_{D^*}$ and $\cos \phi_{D_s^*}$ histograms, we weight each event according to this correction function with a given E_γ . To evaluate the systematic error due to this correction procedure, we vary the correction parameters by one standard deviation obtained from the fit. The maximum difference in the final result is 8%, for which the correction function is shown by the dotted line in figure 3. As a systematic check, we use an exponential function, instead of a polynomial function, as a correction function; this correction function changes the final result by 2%. We also study the $P_{D^{*+}}$ distribution, and use the same procedure to correct it as E_γ , however, the effect is negligible.

We also study the random pion background in the same manner. We use wrong sign combinations from the data and the Monte Carlo as control samples. The effect on the final

result is negligible because the random pion background contribution is small (14% of the total background).

In addition to the above backgrounds, we also take into account feed down from the following decays, $B^- \rightarrow D_1(2420)^0 D_s^{*-}$, $D_1(2420)^0 \rightarrow D^{*+} \pi^-$; $\bar{B}^0 \rightarrow D_1(2420)^+ D_s^{*-}$, $D_1(2420)^0 \rightarrow D^{*+} \pi^0$; $B^- \rightarrow D^{*+} D_s^{*-} \pi^-$; $\bar{B}^0 \rightarrow D^{*+} D_s^{*-} \pi^0$; $\bar{B}^0 \rightarrow D^{*+} D_{s1}(2536)^-$, $D_{s1}(2536)^- \rightarrow \bar{D}^{*0} K^-$, $\bar{D}^{*0} \rightarrow \bar{D}^0 \gamma$; $\bar{B}^0 \rightarrow D^{*+} D_s^{*-}$, $D_s^{*-} \rightarrow D_s^- \pi^0$ [5], $\pi^0 \rightarrow \gamma\gamma$. This contribution is quite small ([1–2] % of the total background), and is estimated as follows. From the measurement of the inclusive $\mathcal{B}(B \rightarrow D_s X)$ and the exclusive $\mathcal{B}(B \rightarrow D^{(*)} D_s^{(*)})$, the sum of the branching fractions for the rest of $B \rightarrow D_s X$ is constrained to be $(2.73 \pm 0.54) \times \mathcal{B}(\bar{B}^0 \rightarrow D^{*+} D_s^{*-})$ [6]. The estimate for the branching fractions for the unknown higher order mode B decays is based on this constraint. We have assumed that the total rate for these higher modes is $(1.1 \pm 1.0) \times \mathcal{B}(\bar{B}^0 \rightarrow D^{*+} D_s^{*-})$. Even if we make the extreme assumption that the rest of the modes making up $B \rightarrow D_s X$ all (or none of them) feed down to the signal mode, the final result changes by less than 2%. The result is very insensitive to the feed-down background because it does not peak in the signal region. We assign large errors ($\sim 90\%$) for the unknown branching fractions. In the fit, the ratio of these feed down backgrounds relative to the signal is fixed, since their branching fractions are estimated relative to the $\bar{B}^0 \rightarrow D^{*+} D_s^{*-}$ decay.

Figures 4(a) and (b) show the fit results when D_s^{*-} and D^{*+} are fully reconstructed, respectively. The data is represented by data points and the fit is represented by the solid histogram. The dashed histogram shows the sum of all backgrounds, and the dotted and hatched histograms show the fake D_s^{*-} (D^{*+}) background and the feed down, respectively. The fits yield $N_{D_s^*} = 76 \pm 11$ and $N_{D^*} = 188 \pm 30$. The normalization of the fake D_s^{*-} (D^0) background is fixed in the fit. The normalization of the other backgrounds are allowed to float. The normalization of the random pion (photon) background obtained from the fit is consistent with the Monte Carlo prediction. This agreement gives further confidence in the Monte Carlo predictions.

To explicitly display the signal, we show the $\cos \phi_{D^*}$ and $\cos \phi_{D_s^*}$ distributions after the all backgrounds are subtracted in figures 4 (c) and (d), respectively. The points are background subtracted data and the solid histogram is the signal function. They are in good agreement. We do not observe any systematic trend outside the signal region.

Table I gives the $R(\epsilon \cdot \mathcal{B})$ for each mode. For the $D^0 \rightarrow K^- \pi^+ \pi^0$ and $\bar{K}^0 \pi^+ \pi^-$ modes, we use the following substitution, $R_j(\epsilon \cdot \mathcal{B})_j = (N_j/N_{K\pi})(\epsilon \cdot \mathcal{B})_{K\pi}$, where N_j is the number of reconstructed D^{*+} 's in the appropriate momentum region in our data sample when the D^0 decay mode j ($= K\pi$, $K\pi\pi^0$ or $K^0\pi\pi$) is used. In this way only the $D^0 \rightarrow K^- \pi^+$ detection efficiency need to be determined from Monte Carlo. We do not use this substitution for

the D_s^- decay modes due to lack of statistics. Substituting all the relevant quantities into equation (1) we obtain,

$$\frac{\mathcal{B}(D_s^- \rightarrow \phi\pi^-)}{\mathcal{B}(D^0 \rightarrow K^-\pi^+)} = 0.92 \pm 0.20 \pm 0.11, \quad (3)$$

where the first error is statistical and the second is systematic. This systematic error includes the uncertainty in the random photon background shape (8%), the uncertainty in the fake D^* and D_s^* background normalization (4%), the uncertainty in the feed down background normalization (2%), the uncertainty in the $R_i(\epsilon \cdot \mathcal{B})_i$ for D_s^- modes (6%), the uncertainty in the $R_j(\epsilon \cdot \mathcal{B})_j$ for D^0 modes (3%), the uncertainty in the tracking efficiency (2%), the error associated with mass cuts (3%), and the uncertainty in the K^0 reconstruction efficiency (1%). Using our measurement of $\mathcal{B}(D^0 \rightarrow K^-\pi^+) = (3.91 \pm 0.19)\%$ [7] we obtain,

$$\mathcal{B}(D_s^- \rightarrow \phi\pi^-) = (3.59 \pm 0.77 \pm 0.48)\%. \quad (4)$$

We take into account the correlation of the systematic errors.

When the D^{*+} is fully reconstructed, we calculate the $\overline{B}^0 \rightarrow D^{*+}D_s^{*-}$ branching fraction independent of the $\mathcal{B}(D_s^- \rightarrow \phi\pi^-)$ to be $\mathcal{B}(\overline{B}^0 \rightarrow D^{*+}D_s^{*-}) = (1.85 \pm 0.30 \pm 0.49)\%$. As a systematic check, we compare this with the measured branching fraction when the $\overline{B}^0 \rightarrow D^{*+}D_s^{*-}$ is fully reconstructed; $(2.11 \pm 0.52 \pm 0.37)\%$ [6,8]. They are in good agreement.

As a systematic check, we have generated 3 sets of 3 million $B\overline{B}$ Monte Carlo events with $\mathcal{B}(D_s^- \rightarrow \phi\pi^-) = 3.7\%$, and analyzed them as if they were data. The results come out as $\mathcal{B}(D_s^- \rightarrow \phi\pi^-) = (3.67 \pm 0.64), (4.00 \pm 0.92)$ and $(4.00 \pm 0.69)\%$. They are consistent with the generated value. We have also looked at other kinematic variables in the partial reconstruction. Using these variables to extract yields, we obtain consistent results for $\mathcal{B}(D_s^- \rightarrow \phi\pi^-)$.

In conclusion, we have made the first statistically significant measurement of $\mathcal{B}(D_s^- \rightarrow \phi\pi^-)$. This result is free of assumptions about the production and decay of charm and bottom mesons, and is $\mathcal{B}(D_s^- \rightarrow \phi\pi^-) = (3.59 \pm 0.77 \pm 0.48)\%$.

ACKNOWLEDGEMENTS

We gratefully acknowledge the effort of the CESR staff in providing us with excellent luminosity and running conditions. J.P.A., J.R.P., and I.P.J.S. thank the NYI program of the NSF, M.S. thanks the PFF program of the NSF, G.E. thanks the Heisenberg Foundation, K.K.G., M.S., H.N.N., T.S., and H.Y. thank the OJI program of DOE, J.R.P., K.H., and M.S. thank the A.P. Sloan Foundation, and A.W., and R.W. thank the Alexander von Humboldt Stiftung for support. This work was supported by the National Science Foundation, the U.S. Department of Energy, and the Natural Sciences and Engineering Research Council of Canada.

REFERENCES

- [1] Particle Data Group, L. Montanet *et al.*, Review of Particle Properties, Phys. Rev. D **50**, 1(1994).
- [2] BES Collaboration, J.Z. Bai *et al.*, Phys. Rev. D **52**, 3781(1995).
- [3] TASSO Collaboration, W. Braunschweig *et al.*, Z. Phys. C **35**, 317(1987), NA14 Collaboration, M. P. Alvarez *et al.*, Phys. Lett. B **246**, 261(1990), ARGUS Collaboration, H. Albrecht *et al.*, Phys. Lett. B **255**, 634(1991), E687 Collaboration, P.L. Frabetti *et al.*, Phys. Lett. B **313**, 253(1993), F. Muheim and S. Stone, Phys. Rev. D **49**, 3767(1994). The reference [1] lists all estimates for $\mathcal{B}(D_s^- \rightarrow \phi\pi^-)$ and describes assumptions made.
- [4] CLEO Collaboration, J. Alexander *et al.*, Phys. Rev. Lett. **65**, 1531(1990), F. Butler *et al.*, Phys. Lett. B **324**, 255(1994), M. Battle *et al.*, Preprint CLEO CONF 94-18.
- [5] CLEO Collaboration, J. Gronberg *et al.*, Phys. Rev. Lett. **75**, 3232(1995), this gives $\mathcal{B}(D_s^{*-} \rightarrow D_s^- \pi^0)/\mathcal{B}(D_s^{*-} \rightarrow D_s^- \gamma) = 0.06 \pm 0.03$.
- [6] CLEO Collaboration, D. Gibaut *et al.*, Preprint, CLNS 95/1354. Accepted by Phys. Rev. D.
- [7] CLEO Collaboration, D. S. Akerib *et al.*, Phys. Rev. Lett. **71**, 3070(1993).
- [8] The value is corrected upward by 4% since this measurement assumed $\mathcal{B}(D_s^{*-} \rightarrow D_s^- \gamma) = 100\%$ and $\mathcal{B}(D_s^- \rightarrow \phi\pi^-) = 3.5 \pm 0.4\%$. The systematic error does not include the error due to $\mathcal{B}(D_s^- \rightarrow \phi\pi^-)$.

FIGURES

3281295-016

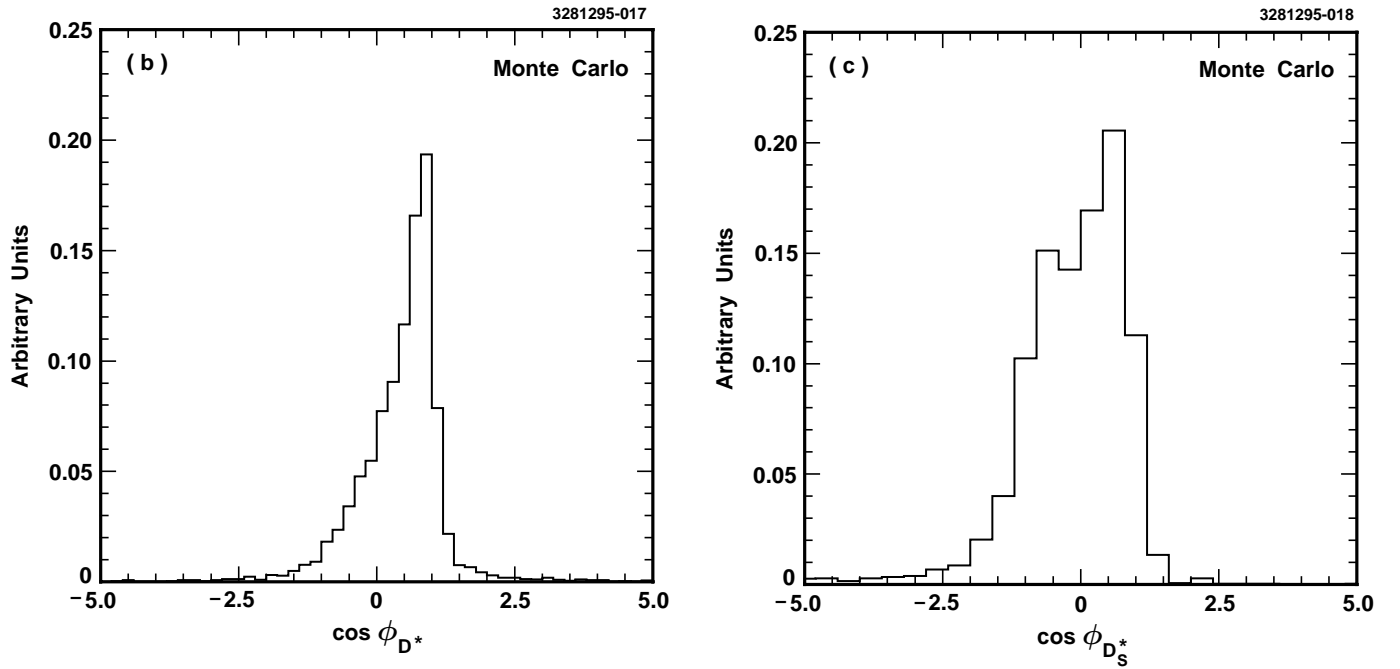
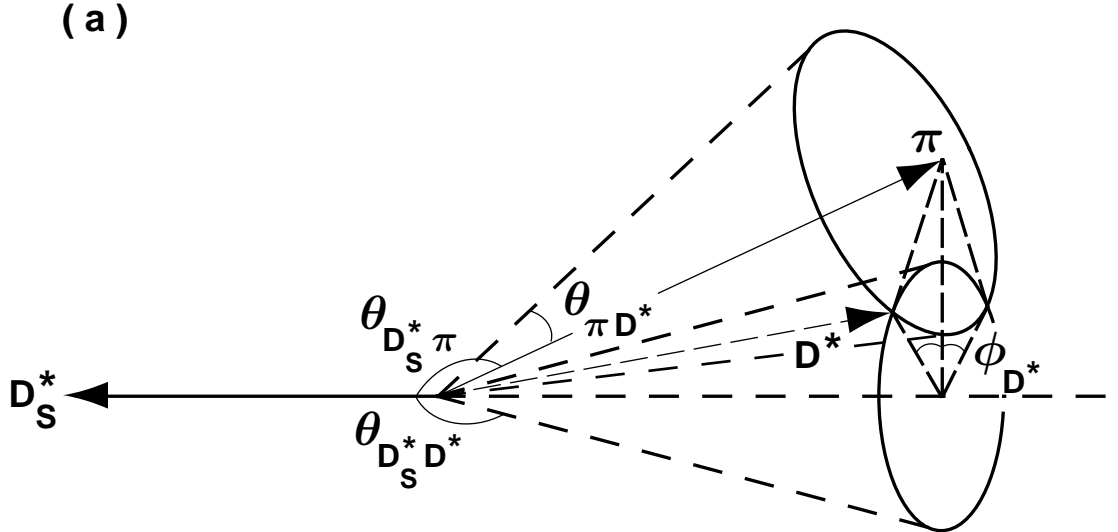


FIG. 1. (a) Partial Reconstruction of the $\bar{B}^0 \rightarrow D^{*+} D_s^{*-}$ decay when the D_s^{*-} is fully reconstructed. (b) The signal Monte Carlo $\cos \phi$ distribution for events in which the D_s^{*-} is fully reconstructed and (c) for events in which the D^{*+} is fully reconstructed.

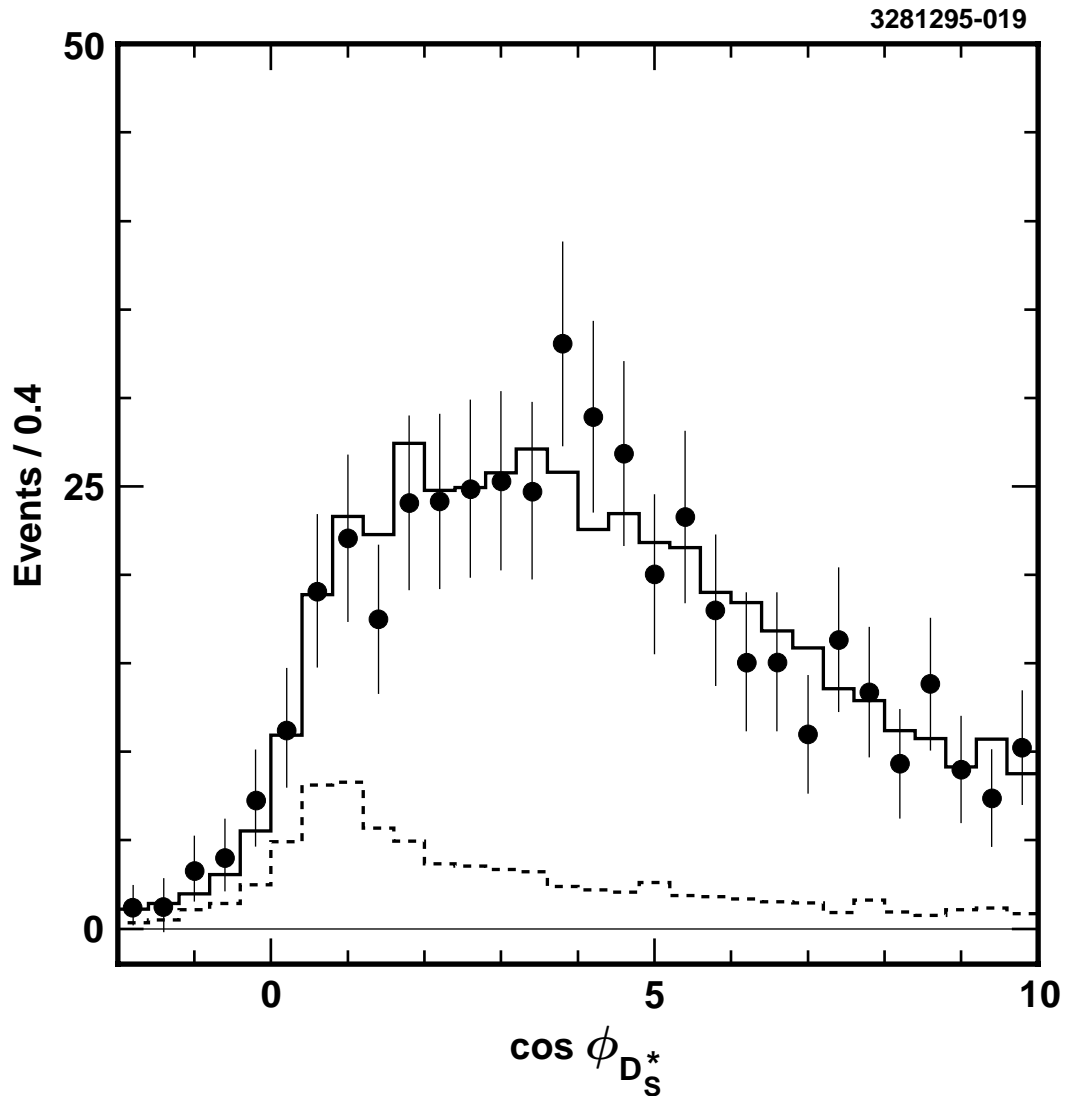


FIG. 2. $\cos \phi_{D^*}$ distribution in $\Delta M_{D_s^*}$ sidebands. The points with errors indicate data and the solid histogram indicates the sum of two Monte Carlo backgrounds. The dashed histogram indicates the contribution from signal pion-fake $D_s^*^-$.

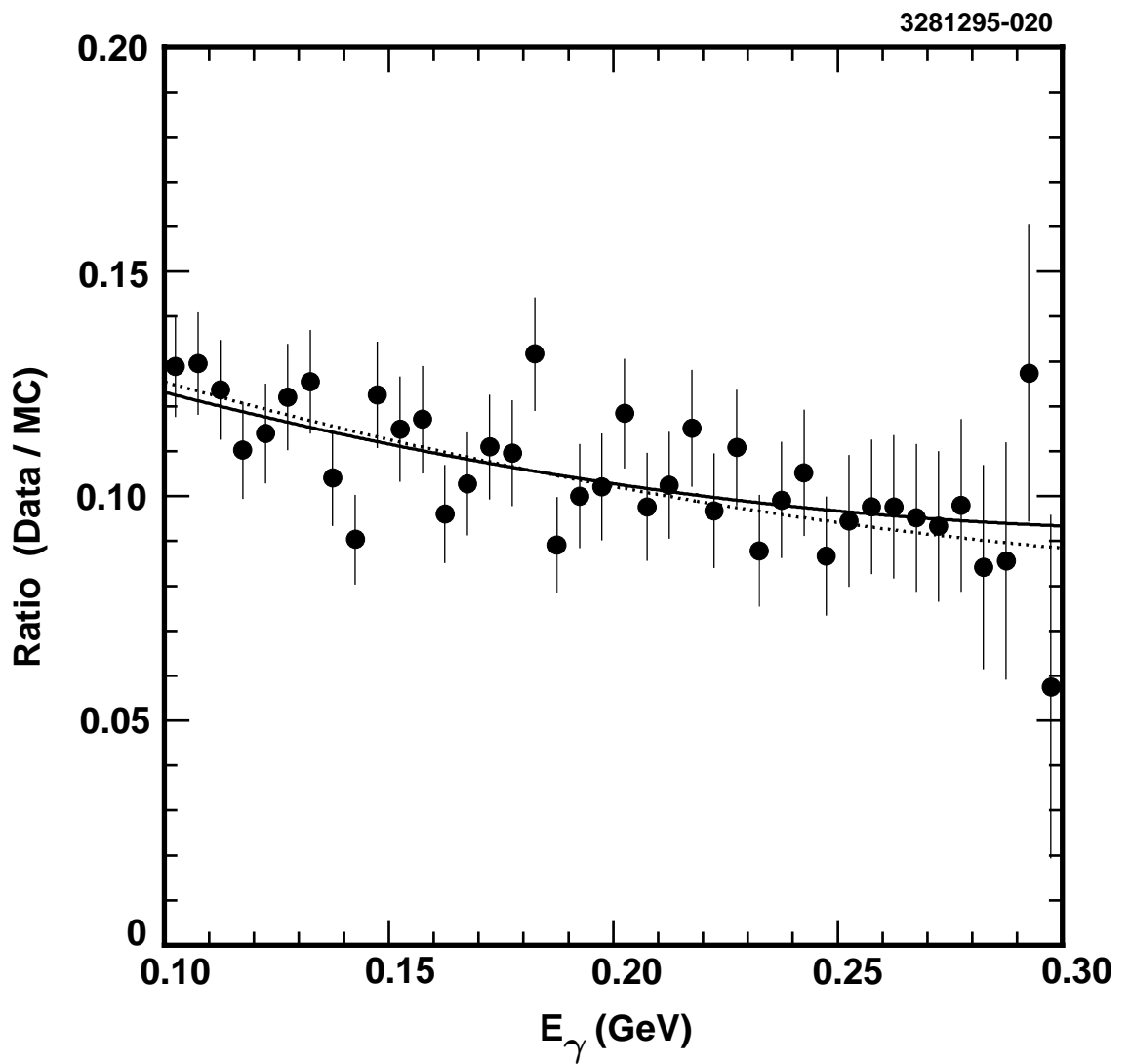


FIG. 3. The ratio of the data to the Monte Carlo in each E_γ bin for random photon background and fit to a second order polynomial function. The dotted line is explained in the text.

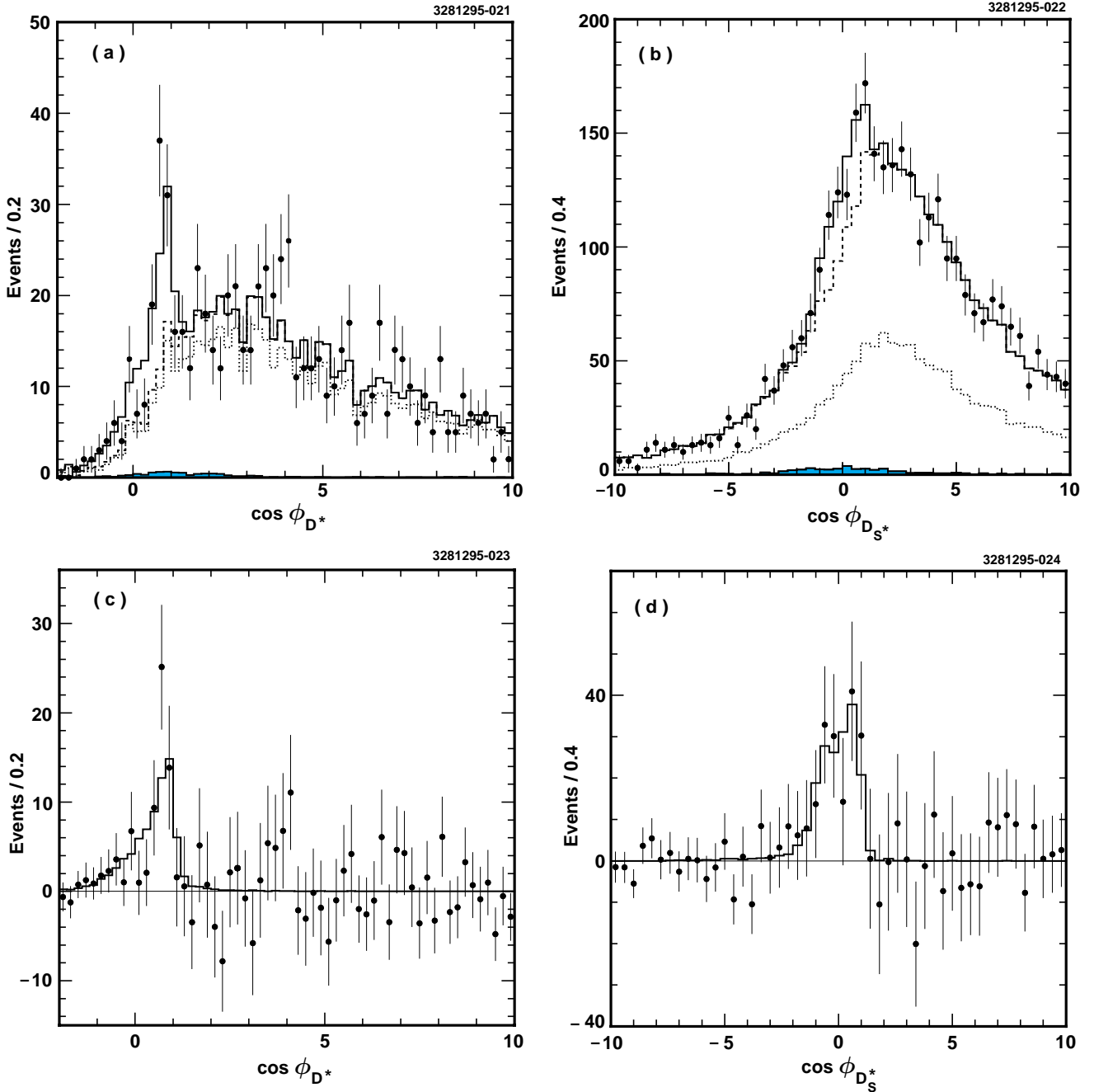


FIG. 4. Fit used to extract the number of \bar{B}^0 candidates when (a) the D_s^{*-} and (b) the D^{*+} are fully reconstructed. The data is represented by data points and the fit is represented by the solid histogram. The dashed line show the sums of all backgrounds, whereas the dotted and hatched lines represent the fake D_s^{*-} (D^{*+}) background and the feed down, respectively. Background subtracted data when (c) the D_s^{*-} and (d) the D^{*+} are fully reconstructed. Solid histograms are signal functions.

TABLES

decay mode	$R(\epsilon \cdot \mathcal{B})$ (%)
$D_s^- \rightarrow \phi\pi^-$	2.34 ± 0.06
$D_s^- \rightarrow K^0K^-$	1.85 ± 0.30
$D_s^- \rightarrow K^{*0}K^-$	2.50 ± 0.27
$D^0 \rightarrow K^-\pi^+$	7.42 ± 0.13
$D^0 \rightarrow K^-\pi^+\pi^0$	6.13 ± 0.35
$D^0 \rightarrow \bar{K}^0\pi^+\pi^-$	1.61 ± 0.14

TABLE I. $R(\epsilon \cdot \mathcal{B})$ when each of the D_s^- and D^0 decay modes is used to fully reconstruct either the D_s^{*-} or D^{*+} , respectively.